

# Magnetic properties of $\text{DyMn}_2\text{Ge}_2$ from Mössbauer and neutron-diffraction studies

G. Venturini and B. Malaman

*Laboratoire de Chimie du Solide Minéral, Université de Nancy I, Boîte Postale 239, 54506 Vandoeuvre les Nancy CEDEX, France*

K. Tomala and A. Szytuła

*Institute of Physics, Jagellonian University, 30-059 Kraków, Reymonta 4, Poland*

J. P. Sanchez

*Centre d'Etudes Nucléaires de Grenoble, Département de Recherche Fondamentale sur la Matière Condensée, 85 X, 38041 Grenoble CEDEX, France*

(Received 15 October 1991)

Neutron-diffraction and  $^{161}\text{Dy}$  Mössbauer measurements on  $\text{DyMn}_2\text{Ge}_2$  are reported. Below 34 K,  $\text{DyMn}_2\text{Ge}_2$  presents a ferrimagnetic structure, while above 40 K an antiferromagnetic order of the Mn moments is inferred. Between 34 and 40 K, these two magnetic phases coexist with an intermediate magnetic phase, the ordered Mn and Dy moments being aligned along the  $c$  axis. The saturation hyperfine parameters reveal a fairly pure  $|\frac{15}{2}\rangle$  ground state, i.e., a Dy moment of  $10\mu_B$ . The experimental data explained in the framework of exchange and crystal-field Hamiltonians allowed us to determine the second- ( $B_2^0$ ) and fourth-order ( $B_4^0$  and  $|B_4^2|$ ) crystal-field parameters as well as the Dy-Dy, Dy-Mn, and Mn-Mn exchange integrals.

## I. INTRODUCTION

The ternary rare-earth  $RT_2X_2$  compounds ( $R$  = rare earth,  $T=3d, 4d,$  or  $5d$  transition metal,  $X=\text{Si, Ge}$ ) were shown to exhibit very exciting physical properties ranging from superconductivity to heavy-fermion behavior.<sup>1,2</sup> Most of them crystallize in the body-centered tetragonal structure of the  $\text{ThCr}_2\text{Si}_2$  type (space group  $I4/mmm$ ) in which the  $R(\text{Th})$ ,  $T(\text{Cr})$ , and  $X(\text{Si, Ge})$  atoms occupy the  $2(a)$ ,  $4(d)$ , and  $4(e)$  sites, respectively. The atoms are arranged in planes stacked perpendicular to the  $c$  axis with the sequence  $R-X-T-X-R$  (Fig. 1). These intermetallics usually order magnetically at low temperatures and present different types of magnetic structures. It has been reported that most of the compounds carry no magnetic moment on the  $T$  atom, while in  $RMn_2X_2$  compounds the Mn sublattice orders magnetically [ferromagnetically or antiferromagnetically (AF)] at relatively high temperatures (300–500 K). An additional magnetic transition,

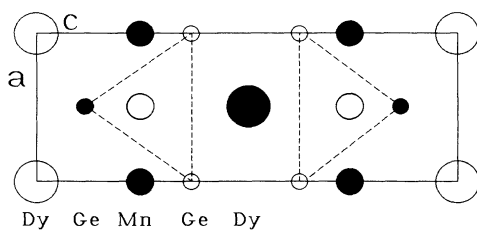


FIG. 1. Crystal structure of  $\text{DyMn}_2\text{Ge}_2$  ( $\text{ThCr}_2\text{Si}_2$  structure type) projected along its  $b$  axis. The solid circles represent atoms at  $y = \frac{1}{2}$ , whereas open circles stand for atoms at  $y = 0$ .

which corresponds to the ordering of the  $R$  sublattice, generally occurs at low temperatures.<sup>2</sup> The magnetic properties of  $\text{DyMn}_2\text{Ge}_2$  have been studied extensively by magnetization measurements on powder samples<sup>3,4</sup> and on single crystals<sup>5,6</sup> and during the completion of this work neutron-diffraction results on the single-crystalline  $\text{DyMn}_2\text{Ge}_2$  sample have been published.<sup>6</sup> It has been shown that, at low temperatures, i.e., below 33 K,  $\text{DyMn}_2\text{Ge}_2$  is a collinear ferrimagnet with ferromagnetic Dy and Mn layers magnetized antiparallel to each other along the  $c$  axis (Fig. 2). In the temperature range from 37.5 to  $T_N=431$  K,  $\text{DyMn}_2\text{Ge}_2$  is a collinear antiferromagnet where only the Mn sublattice is ordered. The Mn moments along the  $[001]$  direction are ferromagneti-

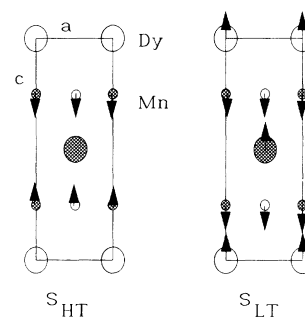


FIG. 2. Magnetic structures of  $\text{DyMn}_2\text{Ge}_2$  at high temperatures: antiferromagnetic phase ( $S_{HT}$ ) and at low temperature: ferrimagnetic phase ( $S_{LT}$ ) as deduced by neutron-diffraction experiments (see text). The structures are projected along their  $b$  axis. The atoms located at  $y = \frac{1}{2}$  are represented by shaded circles and those at  $y = 0$  by open circles. The Ge atoms are omitted for simplicity.

cally coupled on the (001) layers with antiferromagnetic coupling between adjacent Mn layers (Fig. 2). The transition to the AF state at  $T_c = 37.5$  K was shown previously to be of first order.<sup>5</sup> Between 33 and 37.5 K, complex behavior is observed and the occurrence of a new magnetic phase was anticipated but its actual magnetic structure has not yet been determined.<sup>6</sup>

The present study reports on detailed  $^{161}\text{Dy}$  Mössbauer measurements of the temperature dependence of the hyperfine field ( $H_{\text{hf}}$ ) and of the quadrupole coupling constant ( $e^2qQ$ ) at the Dy site in  $\text{DyMn}_2\text{Ge}_2$ . Both hyperfine interaction parameters are sensitive to the nature of the electronic state of the  $\text{Dy}^{3+}$  ions, as fashioned by the magnetic interactions and the crystalline electric field (CEF) produced by the neighboring ions in the lattice. The hyperfine interaction data, when supplemented by bulk magnetization and neutron-diffraction results, are expected to provide information about the strength of the molecular field ( $H_{\text{mol}}$ ) and the crystal-field parameters ( $B_n^m$ ). Furthermore, the magnetic hyperfine field should, in principle, be sensitive to any change of the Mn-sublattice magnetization, via the transferred field contribution to  $H_{\text{hf}}$ , and thus provide insights on the magnetic behavior of  $\text{DyMn}_2\text{Ge}_2$  in 33–37.5-K temperature range. The unexpected occurrence of the coexistence of two magnetic hyperfine subspectra close to 40 K, as shown by the Mössbauer measurements, prompted us to perform, in addition, an extensive neutron-diffraction study of a polycrystalline  $\text{DyMn}_2\text{Ge}_2$  sample in the temperature range from 1.3 to 300 K.

## II. EXPERIMENTAL PROCEDURES

$\text{DyMn}_2\text{Ge}_2$  was prepared by arc melting, under purified argon atmosphere, of stoichiometric amounts of the constituents. Melting was repeated several times in order to ensure homogeneity. Then the sample was vacuum annealed in a silica tube for one week at 800 °C. The sample analyzed by x-ray diffraction using a Guinier camera (Cu  $K\alpha$ ) did not reveal any impurity phase. Lattice parameters at room temperature [ $a = 3.993(1)$  Å,  $c = 10.861(3)$  Å] are in good agreement with earlier published values.<sup>7</sup>

$^{161}\text{Dy}$  Mössbauer spectroscopy measurements were performed using a sinusoidal drive motion of a neutron-irradiated  $^{160}\text{Gd}_{0.5}^{162}\text{Dy}_{0.5}\text{F}_3$  source kept at room temperature. The velocity scale was calibrated using metallic Dy [ $H_{\text{hf}} = 5689(3)$  kOe,  $e^2qQ = 124.9(2)$  mm/s].<sup>8</sup> The absorber thickness was about 45 mg/cm<sup>2</sup> of  $\text{DyMn}_2\text{Ge}_2$ . The  $\gamma$  rays were detected using a high-resolution intrinsic Ge detector. The  $\text{DyMn}_2\text{Ge}_2$  sample was maintained in liquid-helium (nitrogen) cryostats that enable measurements to be made at different temperatures with an accuracy of  $\pm 0.1$  K. The static effective magnetic-field spectra were directly least-squares fitted to the hyperfine parameters by constraining the relative absorption energies and intensities of the Lorentzian lines to the theoretical values.

Neutron-diffraction experiments were carried out at the Institute Laue-Langevin (ILL), Grenoble. The diffraction patterns were recorded with the one-

dimensional curved multidetector D1b at a wavelength  $\lambda = 2.5293$  Å. A special double-wall vanadium sample holder was used in order to minimize neutron absorption. Several patterns were collected between 1.3 and 300 K and special attention was paid to the 30–58-K temperature range where 30 patterns (i.e., 1-K steps) were recorded. No data were collected in the paramagnetic state ( $T_N \sim 440$  K). The first refinements, carried out with the neutron pattern recorded at room temperature, pointed to the occurrence of texture effects (due to the tabletlike shape of the crystallites, the  $c$  axis takes a preferential orientation perpendicular to the neutron beam). In order to correct this effect we followed the suggestion of Dollase<sup>9</sup> and used the March formula:<sup>10</sup>

$$M_{hkl} = \left[ f_{\text{cor}} \cos^2 \alpha + \frac{\sin^2 \alpha}{f_{\text{cor}}} \right]^{-3/2},$$

where  $M_{hkl}$  is a corrective factor for the calculated intensity of each line,  $f_{\text{cor}}$  is a fitted coefficient which reflects the importance of preferential orientation, and  $\alpha$  is the angle between the  $c$  axis and the  $hkl$  plane in Bragg position. The almost constant value of  $f_{\text{cor}} \sim 1.08$ , obtained for all refinements, strongly supports the validity of this correction. Using the Fermi lengths tabulated by Freeman and Desclaux<sup>11</sup> and the magnetic form factor of Mn and  $\text{Dy}^{3+}$  ions taken from Refs. 12 and 13, the scaling factor,  $f_{\text{cor}}$ , the germanium atomic position,  $z_{\text{Ge}}$ , and the magnetic moments of Mn and  $\text{Dy}^{3+}$  were refined by the MiXeD crystallographic executive for diffraction (MXD) least-squares-fit procedure.<sup>14</sup> The MXD program allows one to fit simultaneously the intensities of the nuclear and magnetic reflexions. Attempts to fit the nuclear lines by interchanging the positions of the Mn and Ge atoms always led to a poorer agreement and gave no evidence for any mixing between the Mn and Ge atoms in 4( $d$ ) and 4( $e$ ) sites. Moreover, it is important to emphasize that, because the Mn atoms occupy atomic positions with a C translation lattice mode, the magnetic contributions to the observed intensities, due to a ferromagnetic ordering within the Mn(001) planes, affect only the nuclear lines obeying the extinction rule: ( $hkl$ ) with  $h + k = 2n + 1$ .

## III. NEUTRON-DIFFRACTION STUDY

### A. Experimental results

Neutron-diffraction patterns taken between 1.3 and 300 K clearly show three characteristic temperature ranges (Fig. 3(a)). Below  $T_1 \approx 30$  K, one observes only an increase of the intensities of the nuclear lines. Above  $T_2 = 40$  K, additional lines appear in the neutron-diffraction patterns. Three superlattice lines are superimposed to the lines belonging to the nuclear scattering. There are now no magnetic contributions to the nuclear lines. The Bragg angles of the three superlattice lines can be indexed on the basis of the crystal unit cell as (111), (113), and (201). In the intermediate temperature range,  $34 < T < 40$  K, one observes, besides the above-mentioned superlattice and nuclear lines, four additional lines [Fig. 3(b)] which can be indexed on a tetragonal magnetic unit

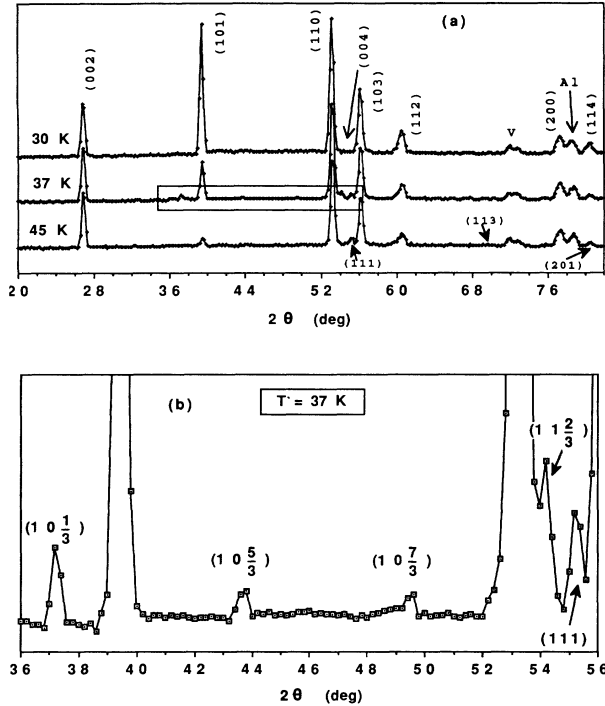


FIG. 3. (a) Neutron-diffraction patterns of DyMn<sub>2</sub>Ge<sub>2</sub> at 30, 37, and 45 K. (b) Detailed view of the neutron-diffraction pattern of DyMn<sub>2</sub>Ge<sub>2</sub> at 37 K showing the occurrence of four extra lines attributed to the  $S_{\text{int}}$  phase (see text).

cell with parameters,  $a' = 3.987(2)$  Å and  $c' = 32.58(1)$  Å roughly equal to  $a$  and  $3c$ , respectively. Furthermore, one should notice that no magnetic contributions to the  $(00l)$  nuclear reflections show up in the whole examined temperature range (1.3–300 K).

The thermal dependences of the intensities of four characteristic peaks, (002), (101), [(111)+(004)], and  $(10\frac{1}{3})$ , are shown in Fig. 4. They demonstrate that (i) the intensity of the (002) line remains constant from 1.3 up to 300 K, (ii) the intensity of the (101) line, whose nuclear contribution is weak (Table I), increases while the intensi-

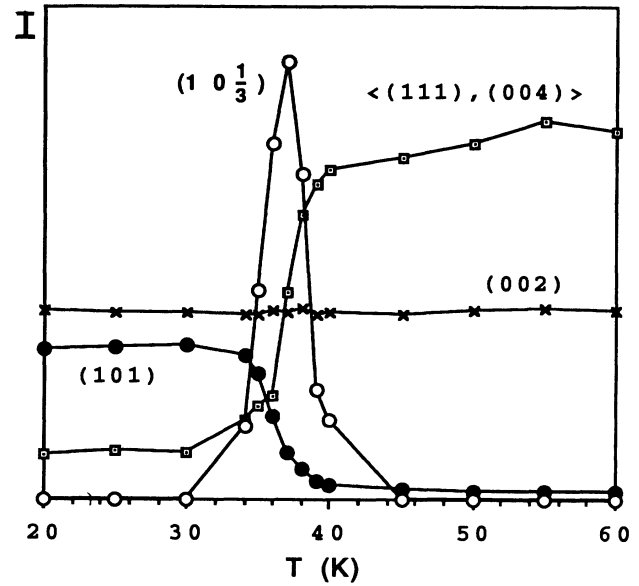


FIG. 4. Temperature dependence of the integrated intensities of the (002), (101), [(111),(004)], and  $(10\frac{1}{3})$  lines.

ty of the [(111)+(004)] line decreases dramatically when lowering the temperature from 40 to 34 K, (iii) the intensity of the  $(10\frac{1}{3})$  line appearing at 40 K and vanishing at 34 K goes through a maximum of about 37 K.

From these results one may conclude that the magnetic moments are always along the  $c$  axis with no major change in the crystal structure. Furthermore, the intensities of the peaks observed below 34 K and above 40 K are in full agreement with the previously reported magnetic structures<sup>6</sup> called, hereafter,  $S_{\text{LT}}$  and  $S_{\text{HT}}$ , respectively. Finally, the data obtained in the range  $34 < T < 40$  K indicates that three magnetic structures ( $S_{\text{LT}}$ ,  $S_{\text{HT}}$ , and  $S_{\text{int}}$ ) coexist in this temperature range, in agreement with the occurrence of a first-order magnetic transition at  $T_c = 40$  K.

TABLE I. Calculated and observed intensities, lattice parameters,  $z_{\text{Ge}}$  atomic position, magnetic moments, and reliability factors at 2 and 45 K. The superlattices lines observed at high temperatures are underscored.

$T = 2$ K			$T = 45$ K		
$a = 3.987(1)$ Å	$c = 10.859(2)$ Å		$a = 3.987(1)$ Å	$c = 10.859(2)$ Å	
$hkl$	$I_{\text{obs}}$	$I_{\text{calc}}$	$hkl$	$I_{\text{obs}}$	$I_{\text{calc}}$
002	420	389	002	410	411
101	1754	1701	101	113	56
110	3850	3909	110	2592	2597
004	21	15	<u>111,004</u>	201	191
103	2048	1991	103	1580	1571
112	903	1000	112	523	444
			<u>113</u>	59	72
200	1236	1290	200	1007	1033
114	985	1047	<u>201,114</u>	288	291
$\mu_{\text{Mn}} = 2.00(27)\mu_B$	$R = 3.7\%$		$\mu_{\text{Mn}} = 1.93(16)\mu_B$	$R = 3.1\%$	
$\mu_{\text{Dy}} = 10.2(2)\mu_B$	$z_{\text{Ge}} = 0.392(1)$			$z_{\text{Ge}} = 0.390(1)$	

## B. Discussion

### 1. Magnetic structure refinement at $T < 34$ K

The present neutron-diffraction results indicate in agreement with the previously published single-crystal neutron study<sup>6</sup> that  $\text{DyMn}_2\text{Ge}_2$  is a collinear ferrimagnet below  $T \approx 34$  K. The magnetic structure of  $\text{DyMn}_2\text{Ge}_2$  consists of ferromagnetic (001) layers of Dy and Mn with the moments along the  $c$  axis and coupled antiferromagnetically (Fig. 2). Table I gives the observed and calculated intensities together with the lattice constants and the refined  $z_{\text{Ge}}$ ,  $\mu_{\text{Mn}}$ , and  $\mu_{\text{Dy}}$  parameters.

At 2 K, the Mn moments are found to amount  $\mu_{\text{Mn}} = 2.00(27)\mu_B$ , in agreement with the value estimated at higher temperature (see below) while the Dy moments are close to the theoretical  $\text{Dy}^{3+}$  free-ion value of  $10\mu_B$ . Furthermore, the temperature dependence of the neutron-diffraction patterns recorded step by step between 34 and 1.3 K indicate that the Dy moments are already fully saturated at 30 K.

### 2. Magnetic structure refinement at $T > 40$ K

The neutron-diffraction data obtained above  $T \approx 40$  K confirm that  $\text{DyMn}_2\text{Ge}_2$  exhibits a simple antiferromagnetic structure where the Dy moments are disordered.<sup>6</sup> The magnetic structure may be described as a stacking of ferromagnetic Mn planes with the Mn moments aligned along the  $c$  axis with the sequence  $+-+-$  (Fig. 2). Notice that this type of magnetic ordering is common to the  $\text{RMn}_2\text{X}_2$  class of materials.<sup>2</sup> Comparison between the observed and calculated intensities of the diffraction peaks at 45 K as well as  $z_{\text{Ge}}$  and Mn magnetic moment values and reliability factor are given in Table I. Moreover, the temperature dependence of the neutron scattering from 300 down to 40 K reveals a continuous increase of the Mn magnetic moments which amount  $1.95\mu_B$  at 40 K, in agreement with the magnetometric measurement.<sup>6</sup> Finally, as shown in Fig. 4, the thermal dependence of the magnetic contribution to the intensity of the (101) reflection allows one to deduce  $T_c = 40(2)$  K for the Dy-sublattice magnetic ordering temperature, in fair agreement with the previously reported values.<sup>3-6</sup>

### 3. Magnetic structure refinement at $34 < T < 40$ K

The diffraction patterns recorded in the intermediate temperature range, i.e., between 34 and 40 K, can be described as a sum of three subpatterns implying the coexistence of three different magnetic phases: (i)  $S_{\text{LT}}$ , the low-temperature phase in which the magnetic contribution affects only the  $(hkl)$  nuclear reflections satisfying the condition  $h+k+l = \text{even}$  (see above), (ii)  $S_{\text{HT}}$ , the high-temperature phase, here, the magnetic ordering of the Mn sublattice only contributes to the occurrence of three superlattice lines  $(hkl)$  with  $h+k+l = \text{odd}$  (see above), (iii)  $S_{\text{int}}$ , the intermediate phase, in which, as shown above, three additional magnetic lines indexed on a magnetic unit cell:  $a' = a$  and  $c' = 3c$  are assigned to  $S_{\text{int}}$ .

The magnetic reflections, attributed to the occurrence

of the  $S_{\text{int}}$  phase, and measured with a rather good accuracy in the 37-K pattern are the superlattice lines  $(10\frac{1}{3})$ ,  $(10\frac{2}{3})$ ,  $(10\frac{7}{3})$ , and  $(11\frac{2}{3})$ . Traces of  $(11\frac{4}{3})$  [obscured by the (103) nuclear reflection] and of  $(10\frac{11}{3})$ ,  $(11\frac{8}{3})$ , and  $\{(11\frac{10}{3}), (10\frac{13}{3})\}$  (overlapping with the vanadium sample holder reflections) are also identified (Table II). All these lines obey the rule  $h+k+l = \text{even}$ . However, despite the high signal-to-noise ratio, no other magnetic reflections with measurable intensities have been detected. The absence of the  $(00l)$  peaks demonstrate that the magnetic moments also aligned along the  $c$  axis in the  $S_{\text{int}}$  phase.

From the above observations, one may conclude that the coupling between the Dy and Mn sublattices is essentially antiferromagnetic. On the other hand, the moment arrangement should be compatible with the  $L$  lattice mode of the magnetic unit cell (tripling of the chemical cell along the  $c$  axis). With these requirements it turns out that the best agreement with the experimental data is obtained with the magnetic structure model shown in Fig. 5. It corresponds to a stacking of ferromagnetic Mn layers along the  $c$  axis with the sequence  $+-++-+$ , i.e., the structure consists of antiferromagnetic and ferromagnetic Mn blocks (Fig. 5). This model requires strong antiferromagnetic Dy-Mn interactions with the ferromagnetic Mn blocks. Paramagnetic Dy layers occur when the nearest-neighbor Dy-Mn interactions are frustrated (i.e., antiferromagnetic blocks). Despite the fact that powder neutron-diffraction experiments do not easily allow one to distinguish between different magnetic structures, this model sounds the most physical owing to the fact that all Mn atoms carry a magnetic moment and to its similarity with the  $S_{\text{HT}}$  and  $S_{\text{LT}}$  phases. It is worth

TABLE II. Calculated and observed intensities,  $z_{\text{Ge}}$  atomic position, magnetic moments (fixed values), relative populations ( $P$ ) of the three coexisting magnetic phases ( $S_{\text{LT}}$ ,  $S_{\text{HT}}$ , and  $S_{\text{int}}$ ), and reliability factor at 37 K. The superlattice lines of the high-temperature  $S_{\text{HT}}$  magnetic phase are underscored.

$hkl$	$I_{\text{obs}}$	$I_{\text{calc}}$
002	420	427
$10\frac{1}{3}$	55	59
101	385	334
$10\frac{5}{3}$	26	37
$10\frac{7}{3}$	31	27
110	2937	3015
$11\frac{2}{3}$	144	135
<u>111,004</u>	113	106
<u>103,11<math>\frac{4}{3}</math></u>	1861	1848
112	553	540
$10\frac{11}{3}$	19	13
$11\frac{8}{3}$	< 10	5
$10\frac{13}{3}$	< 10	9
<u>113</u>	46	36
200	1075	1165
<u>201,114</u>	414	389
$\mu_{\text{Mn}} = 1.95\mu_B$	$P_{S_{\text{LT}}} = 0.29(3)$	$R = 4.3\%$
$\mu_{\text{Dy}} = 10.2\mu_B$	$P_{S_{\text{int}}} = 0.24(1)$	
$z_{\text{Ge}} = 0.389(1)$	$P_{S_{\text{HT}}} = 0.47(3)$	



FIG. 5. Magnetic structure of DyMn<sub>2</sub>Ge<sub>2</sub> in the intermediate phase,  $S_{\text{int}}$ .

noticing that  $S_{\text{int}}$  can be viewed as a “mixing” of the low- and high-temperature magnetic structures.

The thermal dependences of the populations of the different magnetic phases  $S_{\text{LT}}$ ,  $S_{\text{HT}}$ , and  $S_{\text{int}}$  coexisting in the temperature range from 34 to 40 K were estimated assuming this model for  $S_{\text{int}}$  and the same Dy and Mn moments in the three phases.  $\mu_{\text{Mn}}$  was fixed to  $1.95\mu_B$  and  $\mu_{\text{Dy}}$  to its low-temperature value of  $10.2\mu_B$ . The latter assumption is supported by the Mössbauer data (see below). The result of this analysis shown in Fig. 6 in-

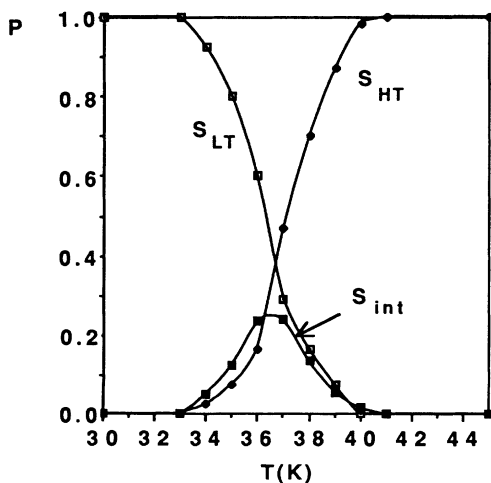


FIG. 6. Temperature dependence of the relative populations ( $P$ ) of the  $S_{\text{LT}}$ ,  $S_{\text{HT}}$ , and  $S_{\text{int}}$  magnetic phases coexisting in the intermediate temperature range, as deduced from neutron-diffraction results.

dicates that the magnetic behavior is dominated by the  $S_{\text{LT}}$  and  $S_{\text{HT}}$  phases whose proportions are strongly temperature dependent. The fraction of the  $S_{\text{int}}$  phase represents, at most, 24%.

Finally, our results may explain the apparent Mn moment reduction (from 2.2 to  $1.2\mu_B$ ) observed by Kobayashi *et al.*<sup>6</sup> at 35 K. Indeed, the  $S_{\text{int}}$  phase, which may occur at different proportion in a single-crystalline sample, was not detected by these authors.

## IV. MÖSSBAUER SPECTROSCOPY STUDY

### A. Experimental results

Figure 7 shows spectra taken at temperatures between 4.2 and 77 K. From 4.2 up to 34 K, the spectra are well analyzed with a single set of hyperfine parameters with the electric field gradient axis parallel to the hyperfine field, i.e., to the magnetization (Table III). Notice that the linewidth is very close to the one observed in metallic dysprosium (4.4 mm/s), thus ruling out hyperfine interaction parameter distributions. Both the hyperfine field ( $H_{\text{hf}}$ ) and the quadrupole coupling constant ( $e^2qQ$ ), as shown in Table III and Fig. 8, fall off smoothly and continuously with increasing temperature. The spectra taken at 38 and 43 K present a superposition of two magnetic hyperfine patterns whose relative intensities change drastically with the temperature (Table III). Figure 7 indicates that it was still possible to fit the data with a static hyperfine Hamiltonian but the severe line broadening of the resonance lines at 43 K indicates the occurrence of relaxation phenomena. They show up clearly in the 50- and 77-K spectra where one observes a progressive collapse of the magnetic hyperfine structure.<sup>15</sup>

### B. Discussion

#### 1. Hyperfine parameters and magnetic structures

The quadrupole interaction and the hyperfine field are commonly described as a sum of several contributions:<sup>16</sup>

$$e^2q_{zz}Q = e^2q_{zz}^{4f}Q + e^2q_{zz}^{\text{lat}}Q, \quad (1a)$$

$$H_{\text{hf}} = H_{\text{hf}}^{4f} + H_{\text{hf}}^{\text{core}} + H_{\text{hf}}^{\text{sp}} + H_{\text{hf}}^{\text{tr,Dy}} + H_{\text{hf}}^{\text{tr,Mn}}, \quad (1b)$$

where  $e^2q_{zz}^{4f}Q$  and  $H_{\text{hf}}^{4f}$  represent the contributions of the localized 4f electrons.  $eq_{zz}^{\text{lat}}$  is the electric field gradient (EFG) produced by the lattice charges. The possible contribution of the conduction electrons is included in  $eq_{zz}^{\text{lat}}$ .  $H_{\text{hf}}^{\text{core}}$  is the core polarization field,  $H_{\text{hf}}^{\text{core}} \simeq -100(g_J - 1)J$  kOe. The other contributions to  $H_{\text{hf}}$  stand for the conduction-electron contributions due to the self-polarization ( $H_{\text{hf}}^{\text{sp}}$ ) induced by the Dy magnetic moment and to the neighboring magnetic atoms, the so-called transferred fields ( $H_{\text{hf}}^{\text{tr,Dy}}$  and  $H_{\text{hf}}^{\text{tr,Mn}}$ ).

The estimate of the 4f contribution to  $e^2q_{zz}Q$  and  $H_{\text{hf}}$  gives useful information concerning the electronic ground state of the Dy<sup>3+</sup> ions. This requires, however, an evaluation of the other contributions described in (1a) and (1b).

For S-state ions (Gd<sup>3+</sup>), the 4f EFG vanishes to zero. This allows the lattice contribution to  $e^2q_{zz}Q$  to be calculated in DyMn<sub>2</sub>Ge<sub>2</sub> from the quadrupole interaction data

TABLE III. Hyperfine interaction parameters for  $^{161}\text{Dy}$  in  $\text{DyMn}_2\text{Ge}_2$ . For  $E_\gamma = 25.6$  keV in  $^{161}\text{Dy}$ :  $1 \text{ mm/s} = 8.5576(10) \times 10^{-8} \text{ eV} = 20.692(2) \text{ MHz} = 0.99307(12) \text{ mK}$ .

$T$ (K)	$H_{\text{hf}}$ (kOe)	(mm/s) $e^2qQ$	$\delta_{\text{IS}}$ (mm/s) <sup>a</sup>	$W$ (mm/s)	Relative intensity
4.2	5918(20)	123.3(1.4)	0.8(2)	5.4(2)	1
12	5921(20)	122.4(1.2)	0.8(2)	5.5(4)	1
18	5929(20)	121.8(1.0)	0.6(2)	4.9(2)	1
25	5897(20)	121.0(1.2)	0.9(2)	4.7(4)	1
34	5873(30)	117.7(1.6)	0.5(2)	4.9(3)	1
38	(1) 5836(40)	116.7(1.6)	0.8(2) <sup>b</sup>	5.2(3) <sup>b</sup>	0.55(4)
	(2) 5279(40)	89.7(2.0)			0.45(4)
43	(1) 5813(40)	119.6(3.2)	1.0(2) <sup>b</sup>	8.5(4) <sup>b</sup>	0.26(3)
	(2) 5254(40)	86.5(1.8)			0.74(6)

<sup>a</sup>Isomer shift relative to the source.

<sup>b</sup>Constrained to the same value for both components.

( $^{155}\text{Gd}$ ) of isostructural  $\text{GdMn}_2\text{Ge}_2$ . It should be mentioned that this procedure does not take into account the possible influence of slightly different lattice parameters. From  $e^2q_{zz}Q = -2.37(3)$  mm/s measured in  $\text{GdMn}_2\text{Ge}_2$  (Ref. 17) and from the known values of the ground-state quadrupole moments  $Q(^{155}\text{Gd}) = 1.30(2)b$  (Ref. 18) and  $Q(^{161}\text{Dy}) = 2.35(16)b$ ,<sup>19</sup> the lattice contribution to the quadrupolar interaction at the  $^{161}\text{Dy}$  nuclei,  $e^2q_{zz}^{\text{lat}}Q(\text{Dy})$ , was estimated to amount to  $-14.4(1.3)$  mm/s. Combin-

ing the experimental  $^{161}\text{Dy}$   $e^2q_{zz}Q$  results with the so-calculated lattice term, one obtains  $e^2q_{zz}^{4f}Q = 137.7(2.7)$  mm/s. This value compares well with the free-ion  $4f$  estimate of 135(1) mm/s obtained from the quadrupolar interaction in cubic  $\text{DyAl}_2$ .<sup>8</sup> This result indicates that the electronic ground state of the  $\text{Dy}^{3+}$  ions in  $\text{DyMn}_2\text{Ge}_2$  at 4.2 K is a pure  $|\frac{15}{2}\rangle$  state. The occurrence of a  $|\frac{15}{2}\rangle$  ground state is in full agreement with the measured free-ion Dy magnetic moment value ( $10\mu_B$ ) and with the easy

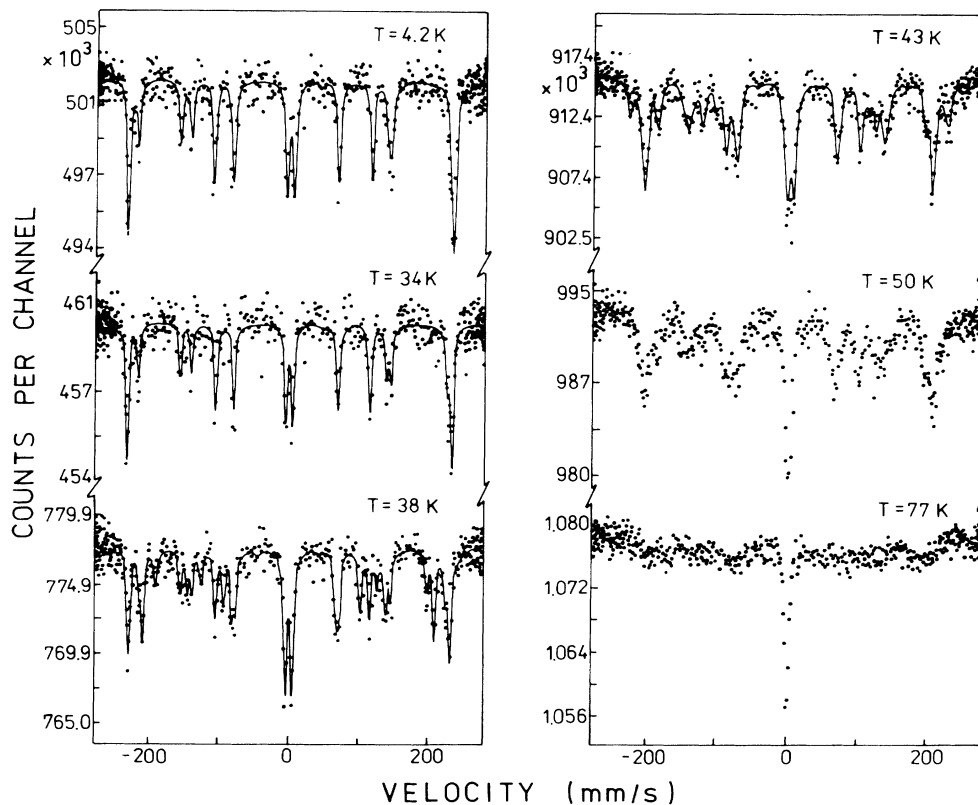


FIG. 7.  $^{161}\text{Dy}$  Mössbauer spectra of  $\text{DyMn}_2\text{Ge}_2$  at different temperatures. The spectra taken at 4.2 and 34 K were fitted with a single component. The spectra recorded at 38 and 43 K were analyzed as a superposition of two magnetic hyperfine patterns using a static Hamiltonian (see text).

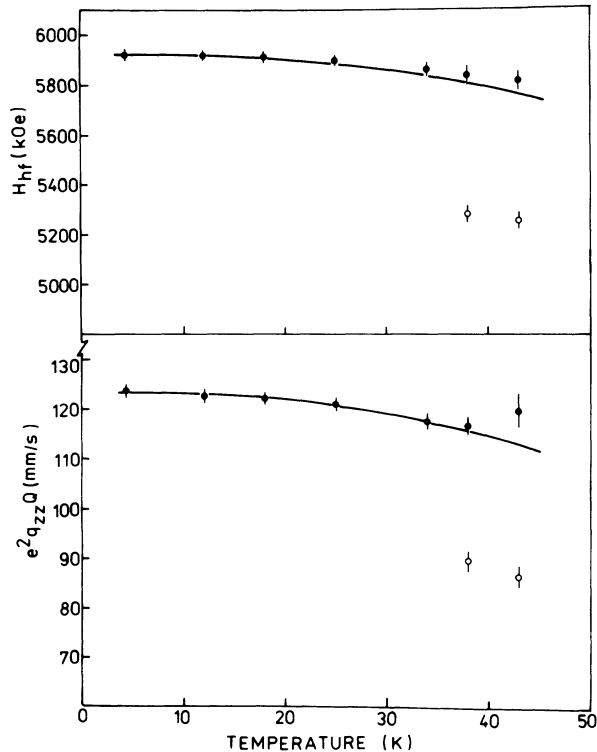


FIG. 8. Temperature dependence of the hyperfine field and quadrupole interaction in DyMn<sub>2</sub>Ge<sub>2</sub>. The solid curves correspond to the results of calculations described in the text. Solid and open circles correspond to the ferrimagnetic and antiferromagnetic phases, respectively.

direction of magnetization along the *c* axis for the Dy sublattice as deduced by the neutron-diffraction data.

Although the  $4f$  contribution to  $H_{hf}$  vanishes in GdMn<sub>2</sub>Ge<sub>2</sub>, a direct evaluation of the  $H_{hf}^{4f}$  contribution in DyMn<sub>2</sub>Ge<sub>2</sub> when scaling the Gd data with the spin  $S = (g_J - 1)J$  factor ( $\frac{5}{7}$ ) is not straightforward in this case.<sup>20</sup> Indeed, in the ferrimagnetic state of DyMn<sub>2</sub>Ge<sub>2</sub> ( $S_{LT}$ ), the transferred field due to the conduction-electron polarization from the Mn atoms is expected to be of the same magnitude in both DyMn<sub>2</sub>Ge<sub>2</sub> and GdMn<sub>2</sub>Ge<sub>2</sub> compounds owing to the fact that the Mn moments are roughly constant along the  $R\text{Mn}_2\text{Ge}_2$  series.<sup>5,21</sup> On the other hand, the transferred field contribution,  $H_{hf}^{tr,Mn}$  in GdMn<sub>2</sub>Ge<sub>2</sub> is difficult to evaluate even when comparing the field measured in GdMn<sub>2</sub>Ge<sub>2</sub> with those obtained in GdT<sub>2</sub>Ge<sub>2</sub> compounds where the transition metal *T* (Fe, Co, Ni, or Cu) does not carry a magnetic moment.<sup>22</sup> This is due to the occurrence of a ferromagnetic ordering of the Gd sublattice in GdMn<sub>2</sub>Ge<sub>2</sub> (Ref. 23) while an antiferromagnetic ordering of the Gd moments is observed in the GdT<sub>2</sub>Ge<sub>2</sub> series.<sup>22</sup> From the <sup>155</sup>Gd hyperfine field results one can only qualitatively conclude that  $H_{hf}^{tr,Mn}$  in GdMn<sub>2</sub>Ge<sub>2</sub> should be notable since the value of  $H_{hf} = -157.5(3.0)$  kOe in GdMn<sub>2</sub>Ge<sub>2</sub> (Ref. 17) is considerably different from those measured in the GdT<sub>2</sub>Ge<sub>2</sub> compounds which vary from  $|H_{hf}| = 248(4)$  kOe in GdCu<sub>2</sub>Ge<sub>2</sub> to  $|H_{hf}| = 300(3)$  kOe in GdNi<sub>2</sub>Ge<sub>2</sub>.<sup>22</sup>

From the above discussion it turns out that any change of the magnetic structure involving the Mn sublattice should influence both the hyperfine field and the quadrupole interaction parameters. Indeed, the actual value of  $H_{hf}$  is directly related to transferred field contribution  $H_{hf}^{tr,Mn}$  [Eq. 1(b)] while any modification of the molecular field acting at the Dy site is expected to modify the  $4f$  contributions  $H_{hf}^{4f}$  and  $e^2q_{zz}^{4f}Q$ . Thus, the smooth variation of the hyperfine parameters observed between 4.2 and 34 K (Table III) allows us to conclude, in agreement with the neutron-diffraction data, that the magnetic structure does not change in this temperature range.

The presence of two magnetic subspectra at 38 and 43 K is to be attributed to the occurrence, as demonstrated previously,<sup>5</sup> of a first-order phase transition at  $T_c \approx 40$  K. Around this temperature the antiferromagnetic ( $S_{HT}$ ) and ferrimagnetic ( $S_{LT}$ ) phases are expected to coexist. This conclusion is strongly supported by the rapid change with temperature of the relative intensities of the two spectral components (Table III). The subspectrum with the largest hyperfine field and quadrupole coupling constant is safely assigned to the low-temperature ferrimagnetic phase ( $S_{LT}$ ) since the values of  $H_{hf}$  and  $e^2qQ$  at 38 and 43 K follow well the temperature dependence of the hyperfine parameters below 38 K (Table III, Fig. 8). This rules out the possibility of any change of magnitude and direction of the Dy and Mn magnetic moments above 34 K as suggested by Kobayashi *et al.*<sup>6</sup> from their single-crystal neutron-diffraction study. Indeed, a decrease of the Dy magnetic moment from  $10\mu_B$  at low temperature to  $6.2\mu_B$  at 35 K should lead to an abrupt falloff of the Dy hyperfine field which is not observed.

The second spectral component with the smaller hyperfine interaction parameters is attributed to the high-temperature antiferromagnetic phase ( $S_{HT}$ ) where the Dy magnetic moments are disordered (here the transferred fields  $H_{hf}^{tr,Mn}$  and  $H_{hf}^{tr,Dy}$  are vanishing and the Dy ions do not feel any molecular field). This is supported by the distinct increase of this component between 38 and 43 K whose overall magnetic splitting remains almost constant up to 50 K (Fig. 7). Notice that long relaxation time for the Dy<sup>3+</sup> ions allows one to observe magnetic hyperfine structure even when these ions are in the disordered (paramagnetic) state.<sup>15</sup>

The relative proportions of the coexisting  $S_{LT}$  and  $S_{HT}$  phases as deduced from the Mössbauer study (Table III) differ somewhat from those determined by our neutron-diffraction data (Table II, Fig. 6). This is not so surprising because the fraction of each phase is strongly dependent on the particle size as well as on the thermal history of the samples used in both types of measurements. Moreover, the occurrence of the  $S_{int}$  phase, although at a rather low level (Fig. 6), is not taken into account in the analysis of the Mössbauer data. This is because the hyperfine parameters originating from the two magnetic Dy sites present in the  $S_{int}$  phase (Fig. 5) cannot be distinguished from those attributed to the  $S_{HT}$  and  $S_{LT}$  phases. This is rather obvious if one considers only the nearest-neighbor Mn surroundings of the Dy ions since the main contribution to the transferred field is expected to come from  $H_{hf}^{tr,Mn}$ .

## 2. Crystal- and molecular-field parameters in DyMn<sub>2</sub>Ge<sub>2</sub>

In the following analysis we will only consider the occurrence of the low- ( $S_{LT}$ ) and high- ( $S_{HT}$ ) temperature magnetic structures. The temperature dependence of  $e^2qQ$  below  $T_c$ , the decrease of the quadrupole coupling constant at  $T_c$ , connected with the disappearance of the molecular field acting at the Dy site, the values of  $H_{hf}$  and  $e^2qQ$  in the  $S_{HT}$  phase as well as the occurrence of a first-order phase transition at  $T_c \simeq 40$  K were explained using exchange-crystal-field Hamiltonians. The Hamiltonians that describe the electronic behavior of the Dy and Mn ions have the following forms:

$$\mathcal{H}_{Dy} = B_2^0 \hat{O}_2^0 + B_4^0 \hat{O}_4^0 + B_4^4 \hat{O}_4^4 - g_{Dy} \mu_B \hat{J}_z H_{mol}(Dy) \quad (2a)$$

$$\mathcal{H}_{Mn} = -g_{Mn} \mu_B \hat{S}_z H_{mol}(Mn) \quad (2b)$$

The crystal-field interaction for tetragonal symmetry was truncated to second- and fourth-order crystal-field  $B_n^m$  parameters (for simplicity,  $B_6^0$  and  $B_6^4$  were set to zero).  $\hat{O}_n^m$  are the Stevens operator equivalents. The magnetic interactions at the Dy and Mn sites are described in the molecular field approximation by the molecular fields  $H_{mol}(Dy)$  and  $H_{mol}(Mn)$ , respectively.  $g_{Dy}$  and  $g_{Mn}$  are the Landé factors and  $\hat{J}_z$  and  $\hat{S}_z$  are the angular momentum operators.

Since we closely follow the calculations of Iwata *et al.*<sup>23</sup> for their molecular-field analysis of GdMn<sub>2</sub>Ge<sub>2</sub>, we introduce their notation for the effective exchange integrals. When  $i, j$  refer to the Dy sites and  $k, l$  to the Mn sites, the exchange constants can be defined as

$$\begin{aligned} J^{Dy-Dy} &= \sum_{j \neq i} J_{ij}, \\ J^{Dy-Mn} &= \sum_i J'_{ik} = \frac{1}{2} \sum_k J'_{ik}, \\ J^{Mn-Mn}(0) &= \sum_{l \neq k} J''_{kl}, \\ J^{Mn-Mn}(\pi) &= \sum_{l \neq k}^0 J''_{kl} - \sum_l^1 J''_{kl} + \sum_l^2 J''_{kl} + \dots, \end{aligned} \quad (3)$$

where  $J_{ij}$ ,  $J'_{ik}$ , and  $J''_{kl}$  are the Dy-Dy, Dy-Mn, and Mn-Mn exchange integrals.  $J^{Mn-Mn}(0)$  refers to the case where the Mn layers are coupled ferromagnetically and  $J^{Mn-Mn}(\pi)$  when the Mn sublattice orders antiferromagnetically with the sequence  $+-+-$  along the  $c$  axis.  $\sum^0$  is the sum over Mn sites in the same basal plane,  $\sum^1$  over Mn sites in the first adjacent planes, and so on. Then, the molecular fields acting on the Dy and Mn atoms can be written as, in the low-temperature ferrimagnetic phase ( $S_{LT}$ ),

$$\begin{aligned} H_{mol}(Dy) &= \frac{(g_{Dy} - 1)^2}{g_{Dy} \mu_B} J^{Dy-Dy} \langle \hat{J}_z \rangle \\ &\quad - \frac{2(g_{Dy} - 1)}{g_{Dy} \mu_B} J^{Dy-Mn} \langle \hat{S}_z \rangle, \\ H_{mol}(Mn) &= \frac{g_{Dy} - 1}{g_{Mn} \mu_B} J^{Dy-Mn} \langle \hat{J}_z \rangle \\ &\quad - \frac{1}{g_{Mn} \mu_B} J^{Mn-Mn}(0) \langle \hat{S}_z \rangle, \end{aligned} \quad (4)$$

in the high-temperature antiferromagnetic phase ( $S_{HT}$ ),

$$\begin{aligned} H_{mol}(Dy) &= 0, \\ H_{mol}(Mn) &= \frac{1}{g_{Mn} \mu_B} J^{Mn-Mn}(\pi) \langle \hat{S}_z \rangle. \end{aligned} \quad (5)$$

Finally, the free-energy  $F$  that arises from the exchange and crystal-field interactions is given as follows:

$$\begin{aligned} F &= -kT \ln Z(Dy) - 2kT \ln Z(Mn) + \frac{1}{2} \langle \mu_{Dy} \rangle H_{mol}(Dy) \\ &\quad + \langle \mu_{Mn} \rangle H_{mol}(Mn), \end{aligned} \quad (6)$$

where  $Z(Dy)$  and  $Z(Mn)$  are the partition functions and  $\langle \mu_{Dy} \rangle$  and  $\langle \mu_{Mn} \rangle$  are the average magnetic moments.

To perform a quantitative analysis of the data, we first evaluated the crystal-field parameters  $B_n^m$ . The  $B_2^0$  term was constrained to the value of  $-1.4$  K obtained from the lattice contribution to the EFG (see Sec. IV B 1) using the relation

$$B_2^0 = \frac{-\alpha_J e q^{\text{lat}} \langle r^2 \rangle (1 - \sigma_2)}{4(1 - \gamma_\infty)} \quad (7)$$

with a selection of atomic parameter values:  $(1 - \gamma_\infty) = 60$ ,  $(1 - \sigma_2) = 0.4$ ,  $\alpha_J = -0.0063$ , and  $\langle r^2 \rangle = 0.2188 \text{ \AA}^2$ .<sup>11</sup> Notice that the Dy moment direction is strongly correlated to the negative sign of  $B_2^0$  which forces the easy direction of magnetization to be along the tetragonal  $c$  axis.

The two other crystal-field parameters,  $B_4^0$  and  $B_4^4$ , were chosen to reproduce the values of the  $4f$  contributions to  $H_{hf}$  and  $e^2qQ$  for the high-temperature antiferromagnetic phase at 38 K. Since, in this case,  $H_{mol}(Dy) = 0$ , the  $4f$  contribution to  $H_{hf}$ , equal to  $(H_{hf} - H_{hf}^{\text{core}} - H_{hf}^{\text{sp}})$ , is estimated to range between 5530(50) kOe ( $H_{hf}^{\text{core}} = 0$ ) and 5400(100) kOe ( $H_{hf}^{\text{sp}}$ , which should be positive, may amount 200 kOe). The value of 104.1(3.3) mm/s for  $e^2q^4fQ$  was obtained from the experimental value of  $e^2qQ$  (Table III) after subtraction of the lattice contribution of  $-14.4(1.3)$  mm/s (see Sec. IV B 1). The value for  $e^2q^4fQ$  and those for  $H_{hf}^4f$ , in the range discussed above, were well reproduced by numerical diagonalization of the Hamiltonian (2a) using positive  $B_4^0$  values ranging from 0.0003 to 0.0008 K and a suitable choice of  $B_4^4$  (0.033–0.024 K). Notice that only the absolute value of  $B_4^4$  can be determined because  $B_4^4$  is related to the anisotropy in the basal plane.

The exchange integral  $J^{Mn-Mn}(\pi)$ , responsible for the magnetic interactions between the Mn moments in the high-temperature antiferromagnetic ( $S_{HT}$ ) phase, can be estimated from the known Néel temperature of 438 K for DyMn<sub>2</sub>Ge<sub>2</sub>.<sup>5</sup> Since the nature (spin or orbital) of the Mn magnetic moment is not known, we assumed following<sup>23</sup>  $S = 1$ , with  $\mu_{Mn}$  at a saturation equal to  $2.2\mu_B$ ,<sup>6</sup>  $g_{Mn}$  was taken to amount 2.2. Then, using the formula

$$J^{Mn-Mn}(\pi) = g_{Mn} \mu_B H_{mol}^{\text{HT}}(Mn) = 3T_N / (S + 1),$$

one deduces  $J^{Mn-Mn}(\pi) = 657$  K. This parameter together with the  $B_n^m$  coefficients determined above allow one to calculate the temperature dependence of the free energy

for the high-temperature antiferromagnetic ( $S_{HT}$ ) phase (curve *b* in Fig. 9).

For the analysis of the data below  $T_c$ , i.e., in the low-temperature phase ( $S_{LT}$ ), the calculations were performed by simultaneously self-consistently diagonalizing the Hamiltonians (2a) and (2b) with molecular fields given by Eq. (4) and the range of crystal-field parameters discussed above. The three exchange integrals,  $J^{Dy-Dy}$ ,  $J^{Dy-Mn}$ , and  $J^{Mn-Mn}(0)$ , were adjusted to fit essentially the temperature dependence of  $e^2qQ$  and the temperature  $T_c$  of the first-order phase transition. Since  $J^{Mn-Mn}(0)$  has no influence on the temperature dependence of the hyperfine parameters because the Mn sublattice magnetization is essentially constant up to  $T_c$ , we first tried to reproduce  $e^2qQ(T)$  with the proper choice of  $J^{Dy-Dy}$  and  $J^{Dy-Mn}$ . Good agreement with the experimental data can only be obtained with positive  $J^{Dy-Dy}$ . This is in contrast with the conclusion obtained by Iwata, Hattori, and Shigeoka<sup>23</sup> from the analysis of their single-crystal magnetization curves of GdMn<sub>2</sub>Ge<sub>2</sub>. Nevertheless, the occurrence of positive  $J^{R-R}$ , i.e., ferromagnetic rare-earth-rare-earth interactions, can be inferred from the magnetic structure of ErMn<sub>2</sub>Ge<sub>2</sub> (Ref. 24) where the ferromagnetic ordering of the Er sublattice is magnetically decoupled from the Mn sublattice which orders antiferromagnetically with the Mn moments along the *c* axis. From the measured Curie temperature of the Er sublattice [ $T_c = 8.5 \pm 3$  K (Ref. 24)] and using the de Gennes scaling,  $T_c \propto (g_J - 1)^2 J(J + 1)$ , we can deduce a hypothetical Curie temperature for the Dy sublattice, induced by the Dy-Dy interactions, of  $T_c^{Dy} = 24 \pm 8$  K. Taking into account that the molecular field produced by the Dy ions is given by

$$g_{Dy} \mu_B H_{mol}^{Dy}(Dy) = 3T_c^{Dy} / (J_{Dy} + 1),$$

we estimated  $J^{Dy-Dy} = 10 \pm 4$  K. It was found that the temperature dependence of  $e^2qQ$  as well as of  $H_{hf}$  is well reproduced with  $J^{Dy-Dy} = 14$  K and  $J^{Dy-Mn} = -30 - 39$  K. The misfit observed at 43 K for  $e^2qQ$  arises from the difficulty to evaluate this parameter when the magnetic subspectrum assigned to the coexisting phase is smeared

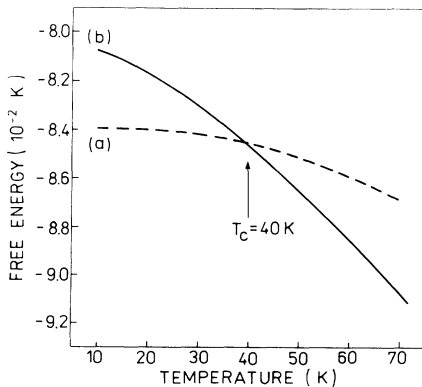


FIG. 9. Temperature dependence of the free energy in the region of  $T_c$  (first order transition) (a) ferrimagnetic phase ( $S_{LT}$ ), (b) antiferromagnetic phase ( $S_{HT}$ ).

TABLE IV. Crystal electric field and exchange parameters which reproduce the quadrupole interaction in the ferrimagnetic state ( $S_{LT}$ ), the first-order phase transition at  $T_c$ , and the hyperfine interaction parameters in the antiferromagnetic state ( $S_{HT}$ ).

Parameter	Value in K
$B_2^0$	-1.4
$B_4^0$	$3-8 \times 10^{-4}$
$ B_4^4 $	$3.3-2.4 \times 10^{-2}$
$J^{Dy-Dy}$	14
$J^{Dy-Mn}$	-(30-39)
$J^{Mn-Mn}(0)$	505-460
$J^{Mn-Mn}(\pi)$	567

out by relaxation effects. On the other hand, the too fast decrease with temperature of the calculated hyperfine field is to be attributed to positive contribution to  $H_{hf}$  which cannot be taken into account properly (see Sec. IV B 1), e.g.  $H_{hf}^{tr,Mn}$  is expected to be temperature independent from 4.2 to 43 K since the strong Mn-Mn interaction keeps the Mn sublattice magnetization constant in this temperature range.

Finally, the exchange integral  $J^{Mn-Mn}(0)$  should range from 505 to 460 K in order to reproduce the occurrence of the first-order magnetic phase transition at 40 K. The value of  $J^{Mn-Mn}(0)$  can be used to estimate a hypothetical Curie temperature,  $T_c^{Mn}$ , for the Mn sublattice. With  $S=1$  one obtains  $T_c^{Mn} = 336-307$  K using the relation  $J^{Mn-Mn}(0) = g_{Mn} \mu_B H_{mol}^{Mn}(Mn) = 3T_c^{Mn}/2$ . This transition temperature should be compared with the one  $T_c^{Mn} \approx 370(10)$  K inferred from the correlation between  $T_c^{Mn}$  and the lattice parameter  $a$ .<sup>25</sup> The temperature dependence of the free energy for the ferrimagnetic ( $S_{LT}$ ) and antiferromagnetic ( $S_{HT}$ ) phases is presented in Fig. 9. The calculated curves were obtained using the following crystal field and exchange parameters (Table IV):

$$B_2^0 = -1.4 \text{ K},$$

$$B_4^0 = 0.0003 \text{ K},$$

$$|B_4^4| = 0.033 \text{ K},$$

$$J^{Dy-Dy} = 14 \text{ K},$$

$$J^{Dy-Mn} = -30 \text{ K},$$

$$J^{Mn-Mn}(0) = 505 \text{ K},$$

and

$$J^{Mn-Mn}(\pi) = 657 \text{ K}.$$

## V. SUMMARY AND CONCLUSIONS

The present work reports the results of neutron-diffraction and <sup>161</sup>Dy Mössbauer studies of DyMn<sub>2</sub>Ge<sub>2</sub>. At low temperature, i.e., below  $T_c \approx 40$  K, DyMn<sub>2</sub>Ge<sub>2</sub> is a collinear ferrimagnet with the Dy and Mn moments, respectively,  $10.2(2)\mu_B$  and  $1.93(16)\mu_B$ , aligned along the *c*

axis. Between  $T_c$  and  $T_N$  ( $\sim 438$  K), the Dy sublattice is disordered and the Mn moments directed along the tetragonal  $c$  axis order antiferromagnetically with the sequence  $+ - + -$ . The magnetic phase transition at  $T_c$  being of first order, one observes between  $\sim 34$  and  $40$  K the coexistence of the ferrimagnetic ( $S_{LT}$ ) and antiferromagnetic ( $S_{HT}$ ) phases together with an intermediate phase ( $S_{int}$ ) whose magnetic structure is depicted in Fig. 5. This shows up in the Mössbauer data by the superposition of two magnetic hyperfine subspectra attributed to the ferrimagnetic and antiferromagnetic phases. For the latter phase, where the Dy magnetic moments are disordered, the occurrence of a magnetic hyperfine structure is due to paramagnetic relaxation effects, i.e., to slowly relaxing  $Dy^{3+}$  magnetic moments. The analysis of the saturation hyperfine field and quadrupole interaction data points to a fairly pure  $|\frac{15}{2}\rangle$  electronic ground state. The

temperature dependences of  $e^2qQ$  and  $H_{hf}$ , of the free energy of the high- ( $S_{HT}$ ) and low- ( $S_{LT}$ ) temperature phases as well as of the occurrence of a first-order transition at  $T_c \simeq 40$  K were explained straightforwardly in the framework of exchange-crystal-field Hamiltonians. This approach enabled us to estimate the exchange integrals (or molecular fields) as well as the second- and fourth-order crystal-field parameters at the Dy atoms in  $DyMn_2Ge_2$ .

#### ACKNOWLEDGMENTS

This work has been partially supported by CPBP 01.12 in Poland. Neutron-diffraction data were recorded at the Institut Laue Langevin (ILL). We are grateful to J. L. Soubeyroux, responsible for the spectrometer used, for his help during the measurements. The Laboratoire de Chimie du Solide Minéral is "Unité Associée au Centre National de la Recherche Scientifique," No. 158.

<sup>1</sup>See, e.g., H. R. Ott and Z. Fisk, in *Handbook on the Physics and Chemistry of the Actinides*, edited by A. J. Freeman and G. H. Lander (North-Holland, Amsterdam, 1987), Vol. 5, p. 85.

<sup>2</sup>A. Szytuła and J. Leciejewicz, in *Handbook on the Physics and Chemistry of Rare Earths*, edited by K. A. Gschneidner, Jr. and L. Eyring (Elsevier, New York, 1989), Vol. 12, p. 133.

<sup>3</sup>K. S. V. L. Narashimhan, V. U. S. Rao, R. L. Bergner, and W. E. Wallace, *J. Appl. Phys.* **46**, 4975 (1975).

<sup>4</sup>A. Szytuła and I. Szott, *Solid State Commun.* **40**, 199 (1981).

<sup>5</sup>T. Shigeoka, *J. Sci. Hiroshima Univ. Ser. A* **48**, 103 (1984).

<sup>6</sup>H. Kobayashi, H. Onodera, Y. Yamaguchi, and H. Yamamoto, *Phys. Rev. B* **43**, 728 (1991).

<sup>7</sup>D. Rossi, R. Mazarra, D. Mazzone, and R. Ferro, *J. Less Common Met.* **59**, 79 (1978).

<sup>8</sup>Y. Berthier, J. Barak, and B. Barbara, *Solid State Commun.* **17**, 153 (1975).

<sup>9</sup>W. A. Dollase, *J. Appl. Cryst.* **19**, 267 (1986).

<sup>10</sup>A. March, *Z. Kristallogr.* **81**, 285 (1932).

<sup>11</sup>A. J. Freeman and J. P. Desclaux, *J. Magn. Magn. Mater.* **12**, 11 (1979).

<sup>12</sup>C. Stassis, H. W. Deckmann, B. N. Harmon, J. P. Desclaux, and A. J. Freeman, *Phys. Rev. B* **15**, 369 (1977).

<sup>13</sup>C. G. Shull and Y. Yamada, *J. Phys. Soc. Jpn.* **22**, 1210 (1962).

<sup>14</sup>P. Wolfers, *J. Appl. Cryst.* **23**, 554 (1990).

<sup>15</sup>H. H. Wickman, in *Mössbauer Effect Methodology*, edited by I. J. Gruverman (Plenum, New York, 1966), Vol. 2, p. 39.

<sup>16</sup>M. A. H. Mac Causland and I. S. MacKenzie, *Nuclear Magnetic Resonance in Rare Earth Metals* (Taylor and Francis, London, 1980).

<sup>17</sup>J. P. Sanchez, K. Tomala, and A. Szytuła, *Solid State Commun.* **78**, 419 (1991).

<sup>18</sup>Y. Tanaka, D. B. Laubacher, R. M. Steffen, E. B. Shera, H. D. Wohlfart, and M. V. Hoehn, *Phys. Lett.* **108B**, 8 (1982).

<sup>19</sup>J. G. Stevens, in *Handbook of Spectroscopy*, edited by J. W. Robinson (Chemical Rubber, Boca Raton, FL, 1981), Vol. 3, p. 403.

<sup>20</sup>K. Tomala, J. P. Sanchez, and R. Kmiec, *J. Phys. Condens. Matter* **1**, 4415 (1989).

<sup>21</sup>E. V. Sampathkumaran, L. C. Gupta, R. Vijayaraghavan, Le Dang Khoi, and P. Veillet, *J. Phys. F* **12**, 1039 (1982).

<sup>22</sup>I. Felner and I. Nowik, *J. Phys. Chem. Solids* **39**, 767 (1978).

<sup>23</sup>N. Iwata, K. Hattori, and T. Shigeoka, *J. Magn. Magn. Mater.* **53**, 318 (1986).

<sup>24</sup>J. Leciejewicz, S. Siek, and A. Szytuła, *J. Magn. Magn. Mater.* **40**, 265 (1984).

<sup>25</sup>H. Fujii, T. Okamoto, T. Shigeoka, and N. Iwata, *Solid State Commun.* **53**, 715 (1985).

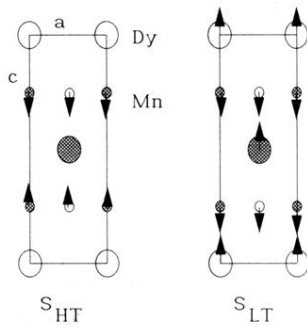


**FIG. 2.** Magnetic structures of DyMn<sub>2</sub>Ge<sub>2</sub> at high temperatures: antiferromagnetic phase ( $S_{HT}$ ) and at low temperature: ferrimagnetic phase ( $S_{LT}$ ) as deduced by neutron-diffraction experiments (see text). The structures are projected along their  $b$  axis. The atoms located at  $y = \frac{1}{2}$  are represented by shaded circles and those at  $y = 0$  by open circles. The Ge atoms are omitted for simplicity.



FIG. 5. Magnetic structure of  $\text{DyMn}_2\text{Ge}_2$  in the intermediate phase,  $S_{\text{int}}$ .